Solid State Communications 179 (2014) 34–38

Contents lists available at ScienceDirect

Solid State Communications

journal homepage: www.elsevier.com/locate/ssc

Electronic parameters and carrier transport mechanism of high-barrier Se Schottky contacts to n-type GaN

V. Rajagopal Reddy [a,b,*], V. Janardhanam [b], Jin-Woo Ju [c], Hyung-Joong Yun [b,d], Chel-Jong Choi [b,**]

[a] Department of Physics, Sri Venkateswara University, Tirupati 517502, India
[b] School of Semiconductor and Chemical Engineering, Semiconductor Physics Research Center, SPRC, Chonbuk National University, Jeonju 561-756, Republic of Korea
[c] LED device Research Center, Korea Photonics Technology Institute, Gwangju 500-779, Republic of Korea
[d] Division of Materials Science, Korea Basic Science Institute, Daejeon 305-333, Republic of Korea

ARTICLE INFO

Article history:
Received 20 May 2013
Received in revised form
14 September 2013
Accepted 4 November 2013
by B.-F. Zhu
Available online 15 November 2013

Keywords:
A. Se Schottky contact
B. Microstructure
C. High Schottky barrier
D. Current transport mechanism

ABSTRACT

The electrical properties and current conduction mechanism of high-barrier Se/n-GaN Schottky diode have been investigated for the first time by current–voltage (*I–V*) and capacitance–voltage (*C–V*) measurements. High resolution transmission electron microscopy (HRTEM) results confirmed that no reaction occurs between Se film and the GaN substrate during Se deposition. Investigations reveal that the contact exhibited an excellent rectification behavior. The estimated barrier height of Se/n-GaN Schottky contact is 0.92 eV (*I–V*) and 1.27 eV (*C–V*) with the ideality factor of 1.10. The barrier height and series resistance are extracted by Cheung's functions. It is observed that the series resistance values obtained from Cheung's functions is in good agreement with each other. Further, capacitance–voltage measurements of the Se/n-GaN Schottky diode are carried out at different frequencies. The discrepancy between Schottky barrier heights obtained from *I–V* and *C–V* measurements is also explained. The AFM results showed that the surface morphology of the Se Schottky contacts on n-GaN is fairly smooth. The forward bias current transport mechanism of the Se/n-type GaN Schottky diode is determined by the log–log plot of *I–V* characteristics. Investigations reveal that the Schottky emission mechanism is found to be dominant in the reverse bias region of Se/n-GaN Schottky diode.

1. Introduction

Group III–V nitride semiconductors, particularly gallium nitride (GaN) based devices are becoming common building blocks in microelectronic and optoelectronics such as light emitting diodes (LEDs) [1], lasers [2], metal–semiconductor–metal (MSM) photo detectors [3], hetero junction field effect transistors (HFETs) [4], high electron mobility transistors (HEMTs) [5], metal oxide semiconductor field effect transistors (MOSFETs) [6] and Schottky rectifiers [7]. The excess reverse bias leakage current is still a major impediment in GaN-based Schottky contacts even though continuous improvement in the synthesis of III–nitride materials by different growth techniques leads to increased device quality. Hence, the characterization and understanding of the properties of metal/GaN contacts are crucial as the performance of GaN-based devices can often be limited by the quality of the ohmic and Schottky contacts [8]. Therefore, the fabrication of Schottky contacts with high barrier height and low reverse leakage current is still a scientific challenge.

For the past few years, several researchers have explored various metal schemes for the fabrication of Schottky contacts on n-type GaN [9–18]. For example, Tian et al. [13] studied the electrical properties of Rh-based Schottky contacts on n-GaN. They found that the Ni/Rh/Au contact exhibits better electrical performance, including a higher Schottky barrier height and lower leakage current compared to the Rh/Au and Ni/Au contacts. Dobos et al. [14] investigated the electrical properties of Au and Ti/Au contacts on n-GaN and the highest Schottky barrier height of 1.07 eV was obtained for as-deposited Au single layer. Fang et al. [15] fabricated the Al/Ni/Au multilayer Schottky contacts on n-GaN, reported that the Al/Ni/Au contact exhibits high quality Schottky contact with a barrier height of 0.875 eV and the lowest

* Corresponding author at: Department of Physics, Sri Venkateswara University, Tirupati 517502, India. Tel.: +91 877 2289472.
** Corresponding author at: School of Semiconductor and Chemical Engineering, Semiconductor Physics Research Center, SPRC, Chonbuk National University, Jeonju 561-756, Republic of Korea. Tel.: +82 63 270 3365.
E-mail addresses: reddy_vrg@rediffmail.com, dr_vrg@rediffmail.com (V. Rajagopal Reddy), cjchoi@chonbuk.ac.kr (C.-J. Choi).

0038-1098/$ - see front matter © 2013 Elsevier Ltd. All rights reserved.
http://dx.doi.org/10.1016/j.ssc.2013.11.011

reverse-bias leakage current respectively after annealing at 450 °C for 12 min in N_2 ambient. Menard et al. [16] fabricated Ni-based Schottky diodes with different thickness (20 nm, 100 nm and 300 nm) on n-type GaN, found that the Ni Schottky contact with a 300 nm thickness shows good rectifying behavior after annealing at 450 °C during 3 min under Argon. Sivapratap Reddy et al. [17] studied the electrical properties of Ni/Pd/n-GaN Schottky diode at different annealing temperatures, found that the highest barrier height (0.81 eV (*I*–*V*), 0.88 eV (*C*–*V*)) was obtained upon annealing at 600 °C. Reddy et al. [18] investigated the electrical properties of Pd/Ru/n-GaN Schottky diode as a function of annealing temperature, reported that the higher barrier height (0.80 eV (*I*–*V*), 0.96 eV (*C*–*V*)) was obtained after annealing at 300 °C. In the literature, it was reported that the barrier height depends on the work function of metals, and reactions between the metals and the GaN substrate. As considering the barrier heights are highly dependent on the metal's work function, selenium (Se) has a high work function (5.9 eV) that makes it ideal for use as Schottky contacts on n-type GaN compared to Pt, Ni, Pd and Au metals. Moreover, Se is much cheaper than Pt, Ni, Pd and Au. Hence, Se can be effectively used to fabricate high-performance and low-cost Schottky devices. Further, there is no report on the electrical characteristics of Se Schottky barriers on n-GaN to date. In this paper, we report the microstructure, electrical properties and current conduction mechanism of Se/n-GaN Schottky contacts for the first time. The electrical characteristics have been measured by current–voltage (*I*–*V*) and capacitance–voltage (*C*–*V*) techniques at room temperature. The forward and reverse current conduction mechanisms of Se/n-GaN Schottky diode are described and discussed.

2. Experimental details

2 μm-thick Si-doped GaN films ($N_d = 4.07 \times 10^{18}$ cm^{-3}) used in this work were grown by metalorganic chemical vapor deposition (MOCVD) on *c*-plane sapphire substrate. First, the n-GaN wafer was ultrasonically degreased with warm trichloroethylene, acetone and methanol for 5 min in each. This degreased layer was then dipped into buffered oxide etch (BOE) solution for 10 min to remove the surface oxide and rinsed in deionized (DI) water. Standard photolithography and lift-off techniques were used to define contact electrodes. To form the ohmic contacts, Ti (30 nm)/Al (60 nm) films were deposited on cleaned GaN surface, followed by annealing at 750 °C in N_2 for 1 min. A Schottky contact of Se (50 nm) films was thermally evaporated from a stainless-steel effusion cell under a base pressure of 1×10^{-6} Torr without substrate heating. The resistivity of the deposited Se layer on n-GaN was found to be 1.17 kΩ cm. The diameter of circular Schottky contacts was 200 μm. The microstructure and interfacial reactions of the Se/n-GaN Schottky contact was investigated by the transmission electron microscopy (TEM) (Tecnai G^2 F30 S-Twin) with an acceleration voltage of 300 kV installed with energy dispersive X-ray spectroscopy (EDX) (EDAX Genesis). Atomic force microscopy (AFM) (Model no: a MOD-1 M plus, Make: Nano focus; Operating mode: Non-contact, tip size < 10 nm) was employed to characterize the surface morphology of Se Schottky contacts. *I*–*V* and *C*–*V* measurements were performed at room temperature using a precision semiconductor parameter analyzer (Agilent 4156C) and precision LCR meter (Agilent 4284A), respectively.

3. Results and discussion

Fig. 1 shows the high resolution transmission electron micrograph (HRTEM) of the interface region between the Se and the GaN substrate. It is observed that there is no reaction between Se film and n-GaN substrate during Se deposition. The selected area electron diffraction (SAED) patterns (insets of Fig. 1) exhibited diffuse halos corresponding to the amorphous phase in the interface region. Furthermore, from the X-ray photoemission spectroscopy results (not shown here), it is observed that there is no shift of the Ga 3*d* peak in the Se/n-GaN interface compared to the Ga 3d peak in the GaN substrate, indicates that no reaction occurring at the interface. The atomic force micrograph (AFM) of the Se/n-GaN Schottky contact is shown in Fig. 2. The surface morphology of the Se Schottky contact is fairly smooth with a root-mean-square (RMS) roughness of 0.184 nm.

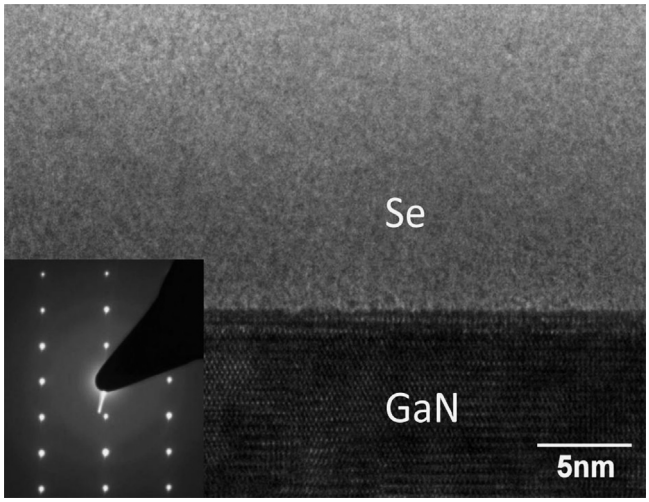

Fig. 1. (Color online) Typical high resolution TEM image for the Se Schottky contact on n-type GaN (SAED patterns are shown in insets).

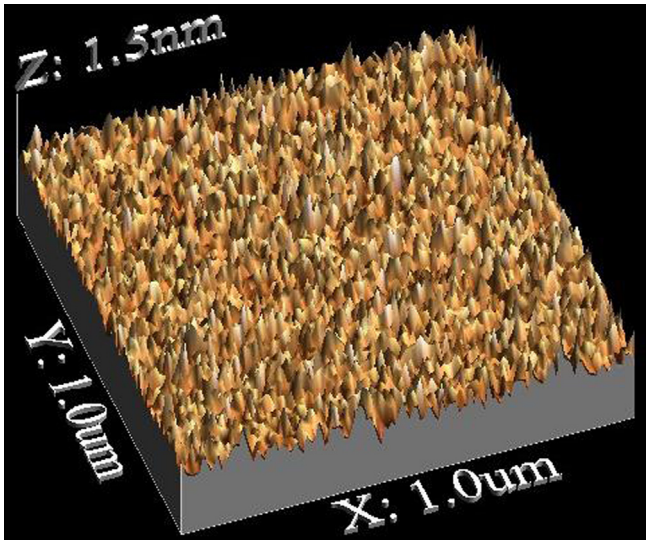

Fig. 2. (Color online) AFM image of the Se Schottky contacts on n-type GaN.

Fig. 3 shows the current–voltage (*I*–*V*) characteristics of the Se/n-type GaN Schottky diode measured at room temperature. The measured reverse leakage current is 3.304×10^{-11} A at −1 V. The rectification ratio of Se/n-GaN Schottky diode is found to be 382 at the bias of 1 V. The Se/n-GaN Schottky diode showed a good rectification behavior, suggests that the current transport over the top of the barrier may be described by the thermionic emission (TE) theory. When the non-ideal Schottky diodes with a series resistance is considered with respect to the forward bias voltages ($V > 3kT/q$), according to the thermionic emission theory, the

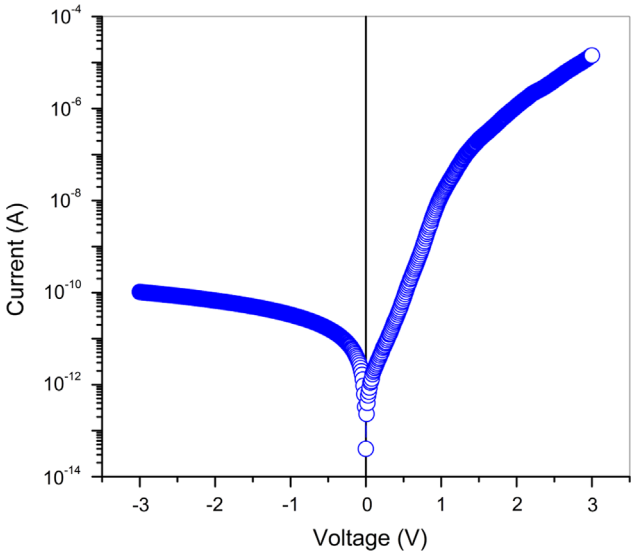

Fig. 3. (Color online) Forward and reverse current–voltage (I–V) characteristics of the Se/n-GaN Schottky diode measured at room temperature.

current across a Schottky diode is given by [19,20]

$$I = I_o \exp\left(\frac{qV_d}{nkT}\right)\left[1-\exp\left(\frac{qV_d}{kT}\right)\right] \quad (1)$$

where $V_d=(V-IR_s)$ is the diode voltage. I_o is the saturation current derived from the straight line intercept of ln (I) at zero-bias and is given by

$$I_o = A^*T^2 \exp\left[\frac{q\phi_b}{kT}\right] \quad (2)$$

T is the absolute temperature in Kelvin, V is the applied voltage, k is Boltzmann's constant, A^* is the effective Richardson constant (26.4 A cm^{-2} K^{-2} for n-GaN) [21], ϕ_b is the zero-bias Schottky barrier height (SBH) and n is the ideality factor. A plot of ln(I) versus V is a straight line with a slope of $q/(nkT)$ and the intercept on y-axis yields I_o. Calculations showed that the barrier height and ideality factor of Se/n-GaN Schottky diode are 0.92 eV and 1.10, respectively. It is noted that the ideality factor is greater than unity. The higher values of ideality factor are probably due to a potential drop in the interface layer and the presence of excess current and the recombination current through the interfacial states between the semiconductor/insulator layers [22]. Another possibility may be due to the presence of a wide distribution of low Schottky barrier height areas caused by a laterally inhomogeneous barrier, as suggested by Werner and Tung [23,24].

Usually, at low voltages the forward bias current–voltage (I–V) characteristics are linear in the semi-logarithmic scale but deviate significantly from linearity due to the effect of series resistance and interface state density when the applied voltage is sufficiently large. The values of barrier height (ϕ_b), ideality factor (n) and series resistance (R_s) can be calculated precisely using the method developed by Cheung [25]. The Cheung's functions are given as

$$\frac{dV}{d(\ln I)} = IR_s + n\left(\frac{kT}{q}\right) \quad (3)$$

$$H(I) = V - n\left(\frac{kT}{q}\right)\ln\left(\frac{I}{AA^*T^2}\right) \quad (4)$$

and

$$H(I) = IR_s + n\phi_b \quad (5)$$

should give a straight line for the data of non-linear (downward curvature) region in the forward bias I–V characteristics. The

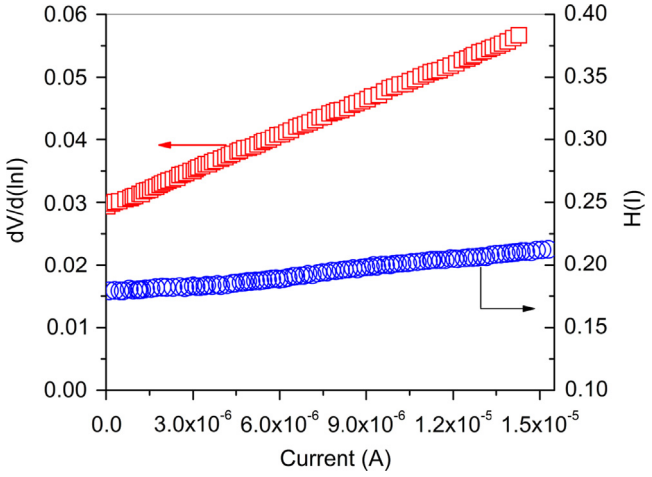

Fig. 4. (Color online) dV/d(ln I) versus I, and $H(I)$ versus I plot of the Se/n-GaN Schottky diode.

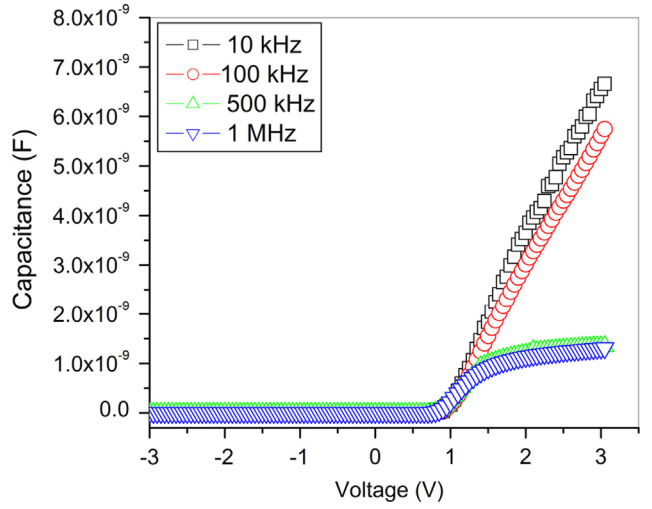

Fig. 5. (Color online) The forward and reverse bias C–V characteristics of the Se/n-GaN Schottky diode measured at room temperature with different frequencies.

experimental dV/d(ln I) versus I, and $H(I)$ versus I plots for the Se/n-GaN Schottky diode are shown in Fig. 4. The values of ideality factor (n) and series resistance (R_s) are found to be 1.12 and 1.9 kΩ from the dV/d(ln I) versus I plot. A plot of $H(I)$ versus I based an Eq. (4) will also give a straight line. The slope of this plot provides a second determination of R_s, which can be used to check the consistency of Cheung's approach. Thus, by using the value of the ideality factor obtained from Eq. (3), the value of barrier height (ϕ_b) can be calculated from the y-axis intercept of the $H(I)-I$ plot. From $H(I)$ versus I plot, ϕ_b and R_s are calculated as 0.94 and 2.3 kΩ respectively. The calculated values of R_s from the plots of dV/d(ln I) versus I are identical to those from the plots of $H(I)$ versus I, implying their consistency and validity. The detailed electrical and structural properties of the Se/n-type GaN structure at different annealing temperatures are under investigation and will be published elsewhere.

Fig. 5 represents the C–V plot for Se/n-GaN Schottky diode at room temperature under various frequencies (10 kHz, 100 kHz, 500 kHz and 1 MHz) as a function of applied bias voltage. It can be clearly seen in Fig. 5, the capacitance decreases with increasing frequency. The increase in capacitance at lower frequencies can be ascribed to the presence of interface states [26]. Because, the interface states follow the alternating current signal at lower

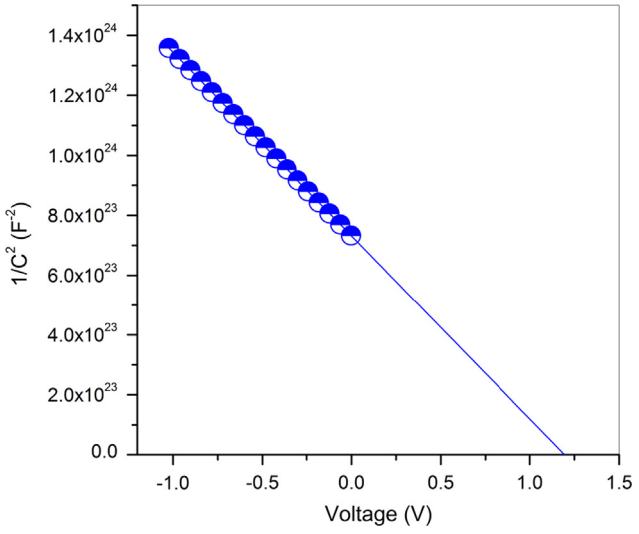

Fig. 6. (Color online) Plot of $1/C^2$ versus V of the Se/n-GaN Schottky diode.

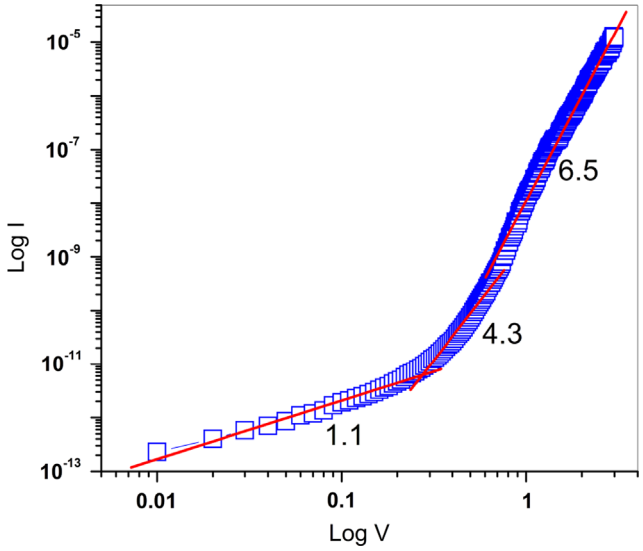

Fig. 7. (Color online) The forward bias log (I) versus log (V) plot of the Se/n-GaN Schottky diode.

frequencies, the interface state capacitance appears directly in parallel with the depletion capacitance which further increases the total capacitance [27]. On the contrary, the interface states are constant at higher frequencies because they cannot follow the alternating signal. As a result, the capacitance is low due to the fact that the interface state charges do not contribute to the diode capacitance [28].

Fig. 6 shows a plot of $1/C^2$ as a function of bias voltage for the Se/n-GaN Schottky diode measured at 1 MHz. The C–V relationship for Schottky diode is given by [20]

$$\frac{1}{C^2}=\frac{2\left(V_{bi}-\frac{kT}{q}-V\right)}{A^2qN_d\varepsilon_s}, \tag{3}$$

where V_{bi} is the flat band voltage, N_d is the donor concentration, A is the area of the Schottky contact and ε_s is the permittivity of the semiconductor ($\varepsilon_s=9.5\ \varepsilon_o$). The x-intercept of the plot of $(1/C^2)$ versus V, V_o is related to the built in potential V_{bi} by the equation $V_{bi}=V_o+kT/q$, where T is the absolute temperature. The barrier height (ϕ_{cv}) is given by the equation $\phi_{cv}=V_{bi}+V_n$, where $V_n=(kT/q)\ln(N_c/N_d)$. The density of states in the conduction band edge is given by $N_c=2(2\pi m^*kT/h^2)^{3/2}$, where $m^*=0.22m_o$ and its value was 2.6×10^{18} cm^{-3} for GaN at room temperature [29]. The extracted barrier height of the Se/n-GaN Schottky diode is 1.27 eV. Results showed that there is a relatively large discrepancy between the Schottky barrier heights obtained by the I–V and C–V techniques. This discrepancy may be due to the existence of Schottky barrier height inhomogeneity at the interface. The current in the I–V measurement is dominated by the current which flows through the regions of low SBH. Hence, the measured I–V barrier height is significantly lower than the weighted arithmetic average of the SBHs [30]. In contrast, the C–V measured barrier height influenced by the distribution of charge at the depletion region boundary and this charge distribution follows the weighted arithmetic average of the SBH inhomogeneity. As a result, the barrier height measured by C–V is close to the weighted arithmetic average of the SBHs. Hence, the SBH determined from the zero-bias intercept assuming thermionic emission as current transport mechanism is well below the C–V measured BH and the weighted arithmetic average of the SBHs [31].

In order to understand the charge transport mechanism of the Se/n-type GaN Schottky diode, a log–log plot of forward I–V characteristics as shown in Fig. 7. The plot shows voltage dependence, followed by power law ($I\propto V^m$, here the exponent m values can be obtained from the slope of Fig. 7) dependence at higher voltages. It is clearly noted from Fig. 7 that the graph exists three different linear regions (1, 2 and 3). In the region 1, at low voltages (up to 0.25 V) the curve is a straight line and the slope value is determined as $m=1.1$, which is close to unity. This indicates that the diode shows an ohmic behavior at low voltages. This is due to existing background doping or thermally generated carriers [32]. In the region 2 (0.26–0.7 V), the slope value is $m=4.4$ which is greater than 2 indicating the charge transport is governed by space charge limited current (SCLC) with a discrete trapping level. In the region 3 (0.71–3 V), the slope of the curve increases as $m=6.5$ because the device approaches the trapped charge limited current (TCLC). Namely, the SCLC conduction should become important when the density of injected free charge carriers is much larger than the thermally generated free charge carrier density [32,33].

Further, it can be clearly seen in Fig. 3, the reverse current increases with increasing bias but it is not saturated. Usually, the reverse characteristics of Schottky diode is dominated by the carrier recombination in the depletion layer and image force lowering of the barrier height as the reverse bias increases the electric field in the junction. By considering Poole–Frenkel emission and Schottky barrier lowering mechanisms across the junction, the reverse leakage current mechanism in the Se/n-GaN Schottky contact has been analyzed. Fig. 8 shows the plots of Poole–Frenkel emission (I_R/E versus $E^{1/2}$) and Schottky emission (I_R/T^2 versus $E^{1/2}$) for the Se/n-GaN Schottky diode. The current through the diode when dominated by Poole–Frenkel effect is given by [34,35]

$$I_R\propto E\exp\left(\frac{1}{kT}\sqrt{\frac{qE}{\pi\varepsilon}}\right) \tag{7}$$

and the lowering of the Schottky barrier is

$$I_R\propto T^2\exp\left(\frac{1}{2kT}\sqrt{\frac{qE}{\pi\varepsilon}}\right) \tag{8}$$

where E is the maximum electric field in the junction. The plots of I_R/E versus $E^{1/2}$ and I_R/T^2 versus $E^{1/2}$ produce a linear curve and their slope can be expressed as [36]

$$S=\frac{q}{nkT}\sqrt{\frac{q}{\pi\varepsilon}} \tag{9}$$

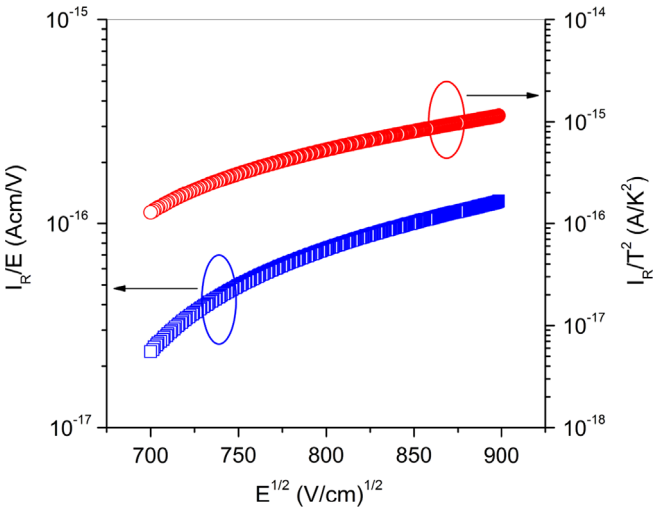

Fig. 8. (Color online) I_R/E versus $E^{1/2}$, and I_R/T^2 versus $E^{1/2}$ plot of the Se/n-GaN Schottky diode.

where $n=1, 2$ for the case of Poole–Frenkel and Schottky emission, respectively. The theoretically calculated slopes obtained from the fits for both Poole–Frenkel emission and Schottky emission are 0.00953 and 0.00477 $(\mathrm{V\,cm^{-1}})^{-1/2}$, respectively. The slope determined from the plot of I_R/E versus $E^{1/2}$ (Fig. 8) is 0.00324 $(\mathrm{V\,cm^{-1}})^{-1/2}$ which is smaller than the theoretical value for Poole-Frenkel emission. This indicates the absence of the Poole–Frenkel mechanism in the Se/n-GaN Schottky contact. On the other hand, the slope determined from the plot of I_R/T^2 versus $E^{1/2}$ (Fig. 8) is 0.00433 $(\mathrm{V\,cm^{-1}})^{-1/2}$ which closely matched with the theoretical value of Schottky emission. Therefore, the results indicate that the Schottky emission is a dominant conduction mechanism in Se/n-GaN Schottky contacts. In this mechanism, the thermally-activated carriers are emitted over the metal–semiconductor barrier under the influence of the electric field, which lowers the barrier height.

4. Conclusion

In conclusion, Se Schottky contact is fabricated on n-type GaN for the first time and its electrical transport characteristics have been investigated using *I–V* and *C–V* techniques. HRTEM results showed that there is no reaction between Se film and GaN film during Se deposition. The Se/n-GaN Schottky contact showed a good rectification behavior. The extracted Schottky barrier height of the Se/n-GaN Schottky contact is 0.92 eV (*I–V*) and 1.27 eV (*C–V*) with the ideality factor of 1.10. The Cheung's method is also employed to determine the barrier height and the series resistance of the Se/n-GaN Schottky diodes. It is noted that the values of series resistance obtained from Cheung's functions are in good agreement with each other. Moreover, *C–V* characteristics of the Se/n-GaN Schottky diode are also measured at different frequencies of 10, 100, 500 and 1000 kHz at room temperature in dark. The difference in barrier height as obtained from *I–V* and *C–V* measurements on Se/n-GaN Schottky diode is attributed to *I–V* and *C–V* techniques to have a different nature. The AFM results indicated that the surface morphology (rms roughness of 0.184 nm) of the Se Schottky contact is fairly smooth. Moreover, the *I–V* characteristic under forward bias is found to be ohmic due to the conduction at low voltage regions. At higher voltage regions there is space charge limited conduction (SCLC) mechanism. Further, the electric field dependence of the reverse current revealed that the Schottky emission is a dominant conduction mechanism in the reverse bias region of Se/n-GaN Schottky diode.

Acknowledgments

This work was supported by the Priority Research Center Program (2011-0031400) and the Converging Research Center Program (2012K001428) through the National Research Foundation of Korea (NRF) funded by the Ministry of Education, Republic of Korea. It was also supported by the R&D Program (Grant no. 10045216) for Industrial Core Technology funded by the Ministry of Trade, Industry and Energy (MOTIE), Republic of Korea.

References

[1] L.C. Chen, C.L. Hsu, W.H. Lan, S.Y. Teng, Solid State Electron. 47 (2008) 1843.
[2] R. Werner, M. Reinhardt, M. Emmerling, A. Forchel, V. Harle, A. Bazhenov, Physica E 7 (2000) 915.
[3] L.B. Flannery, I. Harrison, D.E. Lacklison, R.I. Dykeman, T.S. Cheng, C.T. Foxon, Mater. Sci. Eng. B 50 (1997) 307.
[4] J. Brown, R. Borges, E. Piner, A. Vescan, S. Singhal, R. Therrien, Solid State Electron. 46 (2002) 1535.
[5] J. Moon, M. Micovic, A. Kurdoghlian, P. Janke, P. Hashimoto, W. Wong, L. McCray, C. Nguyen, IEEE Electron. Device Lett. 23 (2002) 637.
[6] D. Mistele, Mater. Sci. Eng. B 93 (2002) 107.
[7] S.J. Pearton, Mater. Sci. Eng. B 82 (2001) 227.
[8] Q.Z. Liu, S.S. Lau, Solid State Electron. 42 (1998) 677.
[9] P. Hacke, T. Detchprohm, K. Hiramatsu, N. Sawaki, Appl. Phys. Lett. 63 (1993) 2676.
[10] K. Suzue, S.N. Mohammad, Z.F. Fan, W. Kim, O. Aktas, A.E. Botchkarev, H. Morkoc, J. Appl. Phys. 80 (1996) 4457.
[11] J.D. Guo, F.M. Pan, M.S. Feng, R.J. Guo, P.F. Chou, C.Y. Chang, J. Appl. Phys. 80 (1996) 1623.
[12] F.D. Auret, S.A. Goodman, G. Myburg, F.K. Koschnick, J.M. Spaeth, B. Beaumon, P. Gibart, Physica. B 273 (1999) 84.
[13] F. Tian, E.F. Chor, Phys. Status Solidi C 5 (2008) 1953.
[14] L. Dobos, B. Pecz, L. Toth, Zs.J. Horvath, Z.E. Horvath, B. Beaumont, Z. Bougrioua, Vacuum 82 (2008) 794.
[15] L. Fang, W. Tao, S. Bo, H. Sen, L. Fang, M. Nan, X. Fu-Jun, W. Peng, Y. Jian-Quan, Chin. Phys. B 18 (2009) 1618.
[16] O. Menard, F. Cayrel, E. Collard, D. Alquier, Phys. Status Solidi C 7 (2010) 112.
[17] M. Siva Pratap Reddy, V. Rajagopal Reddy, I. Jyothi, C.-J. Choi, Surf. Interface Anal. 43 (2011) 1251.
[18] N. Nanda Kumar Reddy, V. Rajagopal Reddy, C.J. Choi, Mater. Chem. Phys. 130 (2011) 1000.
[19] E.H. Rhoderick, R.H. Williams, Metal-Semiconductor Contacts, 2nd ed., Clarendon, Oxford, 1988.
[20] S.M. Sze, Physics of Semiconductor Devices, 2nd ed., Wiley, New York, 1981.
[21] M. Drechsler, Jpn. J. Appl. Phys. 34 (1995) L1178.
[22] D.T. Quan, H. Hbib, Solid State Electron. 36 (1993) 339.
[23] J.H. Werner, H.H. Güttler, J. Appl. Phys. 69 (1991) 1522.
[24] R.T. Tung, Phys. Rev. B 45 (1992) 13509.
[25] S.K. Cheung, N.W. Cheung, Appl. Phys. Lett. 49 (1986) 85.
[26] N. Tugluoglu, F. Yakuphanoglu, S. Karadeniz, Physica. B 393 (2007) 56.
[27] M. Cakar, M. Biber, M. Saglam, A. Turut, J. Polym. Sci.:Part B: Polym. Phys 41 (2003) 1334.
[28] S. Aydogan, M. Saglam, A. Turut, Vacuum 77 (2005) 269.
[29] H.J. Wang, J. Electron. Mater. 27 (1998) 1272.
[30] J.L. Freeouf, T.N. Jackson, S.E. Laux, J.M. Woodal, Appl. Phys. Lett. 40 (1982) 634.
[31] J.P. Sullivan, R.T. Tung, M.R. Pinto, W.R. Graham, J. Appl. Phys. 70 (1991) 7403.
[32] S. Aydogan, U. Incekara, A.R. Deniz, A. Turut, Microelectron. Eng. 87 (2010) 2525.
[33] S. Aydogan, O. Gullu, A. Turut, Phys. Scr. 79 (2009) 035802.
[34] G. Vincent, A. Chantre, D. Bois, J. Appl. Phys. 50 (1979) 5484.
[35] C.H. Han, K. Kim, IEEE Electron Device Lett. 20 (1991) 74.
[36] D.K. Schroder, Semiconductor Material and Device Characterization, 3rd ed., NJ: Wiley, Hoboken, 2006.